Mon. Not. R. astr. Soc. (1980) **192**, 731–743

The interaction between the relativistic jets of SS433 and the interstellar medium

W. J. Zealey *UK Schmidt Telescope of the Royal Observatory Edinburgh, Private Bag, Coonabarabran, NSW 2857, Australia*

M. A. Dopita *Mount Stromlo and Siding Spring Observatories, Private Bag, Woden PO, ACT 2606, Australia*

D. F. Malin *Anglo-Australian Observatory, PO Box 296, Epping, NSW 2121, Australia*

Received 1980 January 16; in original form 1979 November 1

Summary. A sky limited, red sensitive IIIaF plate taken of the field of the W50 supernova remnant reveals two areas of nebulosity, 20 arcmin in extent, centred on SS433 (1909 + 048) and separated from each other by 70 arcmin.

Red spectra at high resolution obtained with the AAT show strong evidence for excitation by low velocity (40–60 km s^{-1}) shocks.

From these data and from morphological considerations we conclude that these optical filaments are excited by the relativistic beams of SS433 and we derive, by two independent techniques, a mass loss rate in the beams of $\sim 3 \times 10^{-6} M_{\odot}$ yr^{-1}. The age of the system is about 10^5 yr.

The data indicate supercritical accretion on to a compact object as the power source of the beams. If this compact object is a black hole it has mass in the range 2–40 $M_{\odot}$ with a probable value of order 12 $M_{\odot}$.

1 Introduction

A search for optical filamentary nebulosity associated with non-thermal radio supernova remnants (SNRs), initiated by Longmore, Clark & Murdin (1977), is being continued using UK Schmidt Telescope plate material (Zealey, Elliott & Malin 1979). Fields south of declination +10° are being searched for nebulosity using both IIIaF + RG630 (Red) and IIIaJ + GG395 (Green) emulsion and filter combinations, covering 630–695 nm and 395–550 nm respectively.

The deep red plates are especially suitable for recording the remnants of older supernovae, which emit predominantly in the lines of Hα, [S II] and [N II]. The IIIaJ plates are useful for identifying younger remnants which emit strongly in the [O III] lines (Goss *et al.* 1979).

As plates become available, overlays generated from the SNR catalogue of Clark & Caswell (1976) are used to locate the non-thermal sources and to define the search areas.

The plates are routinely examined for filamentary nebulosity not associated with known radio remnants.

Where nebulosity is found, a high contrast derivative is made from the original plate, using an unsharp mask to reduce large-scale density variations (Malin 1977). Fine filaments are relatively unaffected by this process and are further enhanced by a subsequent contact copying technique designed to reveal the faintest nebulosity (Malin 1978).

2 The SNR W50 and SS433

The low flux density of the W50 source made it difficult for Clark, Green & Caswell (1975) to derive an accurate spectral index for it. It is only recently (Milne 1979; Geldzahler, Pauls & Salter 1979) that a spectral index of −0.48 has been found, identifying W50 as a non-thermal source. 11-cm polarization maps (Velusamy & Kundu 1974) and beam brightness temperature maps (Geldzahler *et al.* 1979) show the SNR to be a spherical shell, having two extensions to the east and west. A 408-MHz high resolution map (Clark *et al.* 1975) shows only one northern arc of radio emission running east–west. To the south is the point source now identified with the unusually energetic optical source SS433 (Clark & Murdin 1978; Margon 1979). This latter source appears to be ejecting material at velocities of up to 40 000 km s^{-1}.

The deep UKSTU red plates taken on 1979 June 3 and searched two days later show two arcs of filamentary nebulosity, each 20 arcmin in extent and separated by 70 arcmin. These lie almost equidistant from the SS433 source (Plate 1). The positions of both of these filaments, independently discovered by van den Bergh (1979) and of SS433 are given in Table 1.

The eastern filament is the brighter of the two and is just visible on the National Geographic–Palomar Sky Survey red prints. It is clearly seen in Plate 1, made from a deep IIIaF/RG630 plate. Both filaments run approximately parallel to the galactic plane and appear to be separated by a lane of obscuration which runs north–south across the field. The 11-cm polarization vectors (Velusamy & Kundu 1974) are aligned with the filaments, which lie within the radio contours of W50.

The high quality 2695 MHz map of W50 which has recently become available (Geldzahler *et al.* 1979) shows a wealth of detail. A simplified version of this map is presented in Fig. 1 to show the relation of the optical filaments with the radio source. W50 is revealed as a shell-type source with an unusually high level of emission in the inner parts. It has ansae east and west, of which the eastern is of lower surface brightness and it is more extended. SS433 is almost exactly in the centre of inner slightly elliptical shell, and the optical filaments continue this shell in the vicinity of the ansae. This is important as it indicates that the ansae have developed from an earlier elliptical shell-type structure.

Optical spectra were obtained on the 3.8-m Anglo-Australian telescope on the night of 1979 August 15 in the red part of the spectrum (6200–7500 Å). The instrument used was

Table 1. Log of the AAT spectrophotometric observations.

Position identification	RA (1950.0) hr	min	s	Dec °	′	″	UT 1979 Aug. 15	Integration time (s)
SS433	19	09	21.3	+04	53	54	10:55	300
W50#1 (East)	19	11	52.1	+04	57	02	11:06	900
Sky	19	12	52.2	+04	57	01	11:23	900
W50#2 (West)	19	07	17.3	+05	02	18	11:47	900
W50#3 (West)	19	07	09.7	+04	56	20	12:06	900

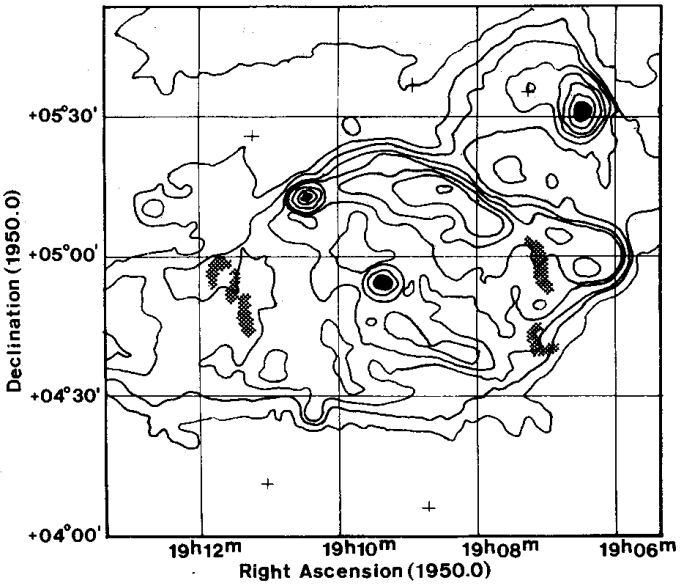

Figure 1. The relationship of the optical filaments to the radio shell (Geldzahler *et al.* 1979).

the IPCS (Boksenberg 1972; Boksenberg & Burgess 1973) mounted on the RGO spectrograph. The grating has 1200 line mm^{-1} and is blazed at 7500 Å. This was used to blaze the collimator in the first order with a GG495 filter. The slit width was 200 μm, and aperture broadening effects matched the grating resolution giving a spectral resolution of 46 km s^{-1} at Hα. The external memory was used, giving in a single frame 20 spectra each 2044 pixels long separated by 4.15 arcsec projected on the sky.

Three brighter regions were selected for study, given in Table 1. To optimize signal to noise in the reduction to relative line intensities given in Table 2, the following reduction procedure was used. Spectra in a given frame were first added giving each a weight proportional to the nebular signal in it. A similarly weighted sky frame was then subtracted, and the result divided by a similarly weighted 'flat field' frame to remove microstructure. Conversion to absolute flux $Å^{-1}$ was made using observations of the Oke (1974) standard Van Maanen 2 in a wide slit (5 arcsec) mode.

The radial velocity data of Table 3 are taken from a simple addition of all spectra in a given frame. The wavelength calibration for each spectrum is obtained from measurement of the Meinel OH band lines in the airglow, to be specific, the OH 6–1 P-branch lines (Chamberlain 1961). It is internally consistent to ±0.05 Å.

Table 2. Spectrophotometry of the W50 filaments.

Ion identification	Wavelength Å	Relative intensity (Hα = 100.0) W50#1 (east)	W50#2 (west)	W50#3 (west)
[O I]	6300	128 ± 20	18 ± 30	30 ± 30
[O I]	6363	57	22	–
[N II]	6548	94	84	56
Hα	6563	100 ± 4	100 ± 8	100 ± 12
[N II]	6584	308	260	175
[S II]	6717	114	121	72
[S II]	6731	77	88	74
[O II]	7319	11	7	20
[O II]	7330	20 ± 10	33 ± 10	28 ± 15

Table 3. Radial velocities and velocity dispersions in the W50 filaments.

Region	V_{LSR} (km s^{-1})		$\langle V^2 \rangle^{1/2}$ (km s^{-1})	
	Hα	N II	Hα	N II
W50#1 (E)	+126(±6)	+127(±10)	78(±15)	65(±15)
W50#2 (W)	+80(±10)	+85(±10)	79(±15)	51(±20)
W50#3 (W)	+72(±12)	+90(±15)	88(±15)	60(±18)

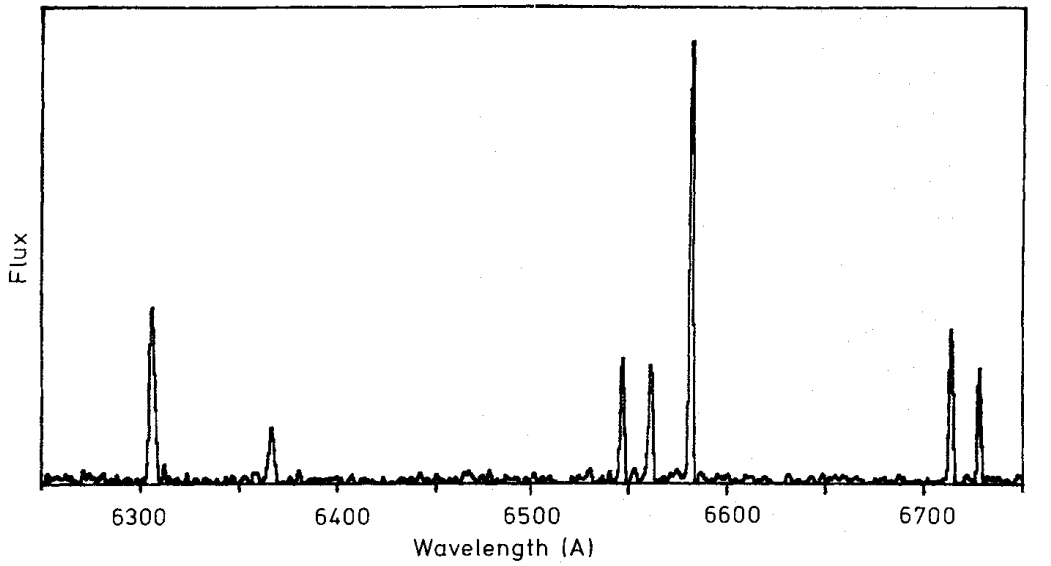

Figure 2. The spectrum of W50E between the [O I] λ6300 Å line and the [S II] λ6717, 6731 Å doublet.

The striking characteristics of the observed spectra (*cf.* Fig. 2) are the very great strength of the [N II] and [S II] lines with respect to Hα (independently discovered by Murdin & Clark 1979) and the relatively modest velocity dispersions observed. Although the gas is almost certainly shock excited, the velocity dispersions are very low (40–60 km s^{-1}), in contrast to Pup A, a SNR with similar strength of the [N II] lines but which has a very large (~300 km s^{-1}) velocity dispersion (Dopita, Mathewson & Ford 1977).

We will now attempt to interpret these optical data and the published radio data on W50 in a manner which is consistent with the observed properties of SS433.

3 Dynamic models for W50

Crucial to the energy requirements of any model to describe the SS433/W50 system is an estimate of the distance. If we assume that the radio and optical structures are the result of a normal supernova event, an estimate of the distance can be made using the usual Σ–d relation for SNRs. Such estimates yield distances in the range $1600 \leqslant d \leqslant 3300$ pc (Large 1970; Caswell & Lerche 1979; Milne 1979). Such a simplistic approach might be questioned on account of the peculiar morphology of W50 and the presence of such a remarkable central object. From optical observations of SS433, Margon *et al.* (1979) find that the structure of the interstellar absorption lines suggest a distance in excess of 3.5 kpc. The radial velocities of the optical filaments can be used to estimate a distance. If only the dense western filaments are considered, the kinematic distance is 5–7 kpc (if the Sun is at 10 kpc from the Galactic Centre). However, this is not considered reliable because locally measured velocities may not be representative of the whole object. Finally, we might anticipate the results obtained below, where, from a consideration of the asymmetry of the ansae, we estimate a distance of 6 kpc.

From all of this, we may conclude almost certainly that the system lies between 2 and 6 kpc, with (in the authors' opinion) a probable value lying closer to upper value.

The optical dimension of W50 in the east–west direction is 70 arcmin. The radio map of Geldzahler *et al.* (1979) gives an east–west extent of the ansae of 110 arcmin and a north–south dimension of 45 arcmin. Ryle *et al.* (1978) found a similar asymmetry in the radio dimensions and derived a major diameter of 81 arcmin and a minor diameter of 45 arcmin. Such an asymmetry could be caused by expansion into the interstellar medium with a density gradient (Kompaneets 1960; Caswell 1977), an idea supported by the fact that the major axis is directed out of the galactic plane and by the observation of an [S II] ratio above the low density limit in the western filaments closer to the galactic plane. However, if, as we believe, SS433 is associated with W50, the almost central position of this source makes such an interpretation unlikely. For an asymmetry of the size observed, a Kompaneets solution would place the explosion centre nearer the western filaments in the appropriate ratio of distances 1:3.6, or displaced by 24 arcmin from the radio centre towards the west. In fact, it is only displaced by 2.7 arcmin which would demand a transverse proper motion of SS433 towards the east which almost exactly compensates the asymmetric expansion.

3.1 SNR PLUS STELLAR WIND

A simpler hypothesis to explain the morphology of W50, mentioned by Geldzahler *et al.* (1979), would be to invoke the ram pressure of the relativistic steams of SS433 as a way of generating the asymmetry. The expansion north–south is determined by the pressure in the supernova remnant, whilst in the east–west direction this is supplemented by the pressure of the relativistic steams leading to more rapid expansion.

Abell & Margon (1979) and Martin, Murdin & Clark (1979) have produced a dynamical model for the jets which gives a solution for the velocity, v, the mean angle of inclination of the beam axes to the line-of-sight, i, and the obliquity of the beams to this axis, θ, as they precess about it. The solution is ambiguous, but gives $v = 0.27c$, $i = 78°$ or $17°$ and $\theta = 17°$ or $78°$. Since the clearly defined optical filaments to the east subtend just over $30°$ at SS433 we prefer the first of these solutions.

Following Kompaneets (1960), the velocity of a shock front is

$$V_s = \left[P/\rho_0^2\left(\frac{1}{\rho_0} - \frac{1}{\rho_1}\right)\right]^{1/2} \tag{3.1}$$

where P is the pressure and ρ_0, ρ_1 are the densities ahead and behind the shock respectively. For a strong shock, the denominator is $3\rho_0/4$ and the pressure for a supernova shock is given by:

$$P = (\gamma - 1)\epsilon \tag{3.2}$$

where ϵ is the energy density at the shock and γ is the ratio of specific heats. In the Kompaneets formulation:

$$P = (\gamma - 1)3\lambda E/r^3$$

where λ is assumed constant and E is the energy per steradian deposited by the supernova explosion.

Substituting in equation (3.1) gives:

$$V_s = \left[\frac{4(\gamma - 1)\lambda E}{\rho_0}\right]^{1/2} r^{-3/2} = \alpha^{1/2} r^{-3/2}. \tag{3.3}$$

This solution must be identical to the Sedov (1959) solution, hence

$\gamma(\lambda - 1) = 0.5912.$

Consider now the stellar wind contribution. This gives an extra pressure term

$$P = \dot{M}_* V_* / r^2 \tag{3.4}$$

where V_* is the wind velocity (=0.27c in our case) and $\dot{M}_*$ is the relativistic mass loss per steradian. Hence (3.1) becomes

$$V_s = (\alpha/r^3 + \beta/r^2)^{1/2} \tag{3.5}$$

where

$\beta = 4\dot{M}_* V_* / 3\rho_0.$

The integral with time is therefore

$$t = \int_0^r \frac{r\,dr}{(\beta r + \alpha)^{1/2}} \tag{3.6}$$

which can be reduced to a standard form to give the analytic solution:

$$t = \frac{\alpha^2}{2\beta^{5/2}}\{(1-u)^{1/2}u^{1/2}(u - 3/2) + 3/2 \ln [u^{1/2} + (1+u)^{1/2}]\} \tag{3.7}$$

where

$u = \beta r/\alpha.$

This solution is given in Fig. 3 for the dimensionless radius u and the dimensionless time $B = 2\beta^{5/2}\alpha^{-2}t$. From the diagram it is evident that at small r, the supernova explosion pressure term dominates giving a standard Sedov solution. This can be proven by a tedious expansion of (3.7) at the limit $\beta \to 0$. For large r, the stellar wind pressure wins.

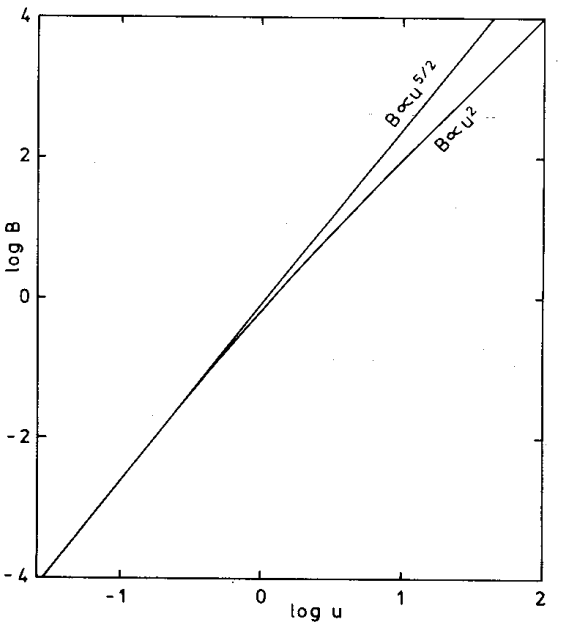

Figure 3. The dimensionless time B against the dimensionless radius u for the stellar wind assisted supernova remnant model described in the text.

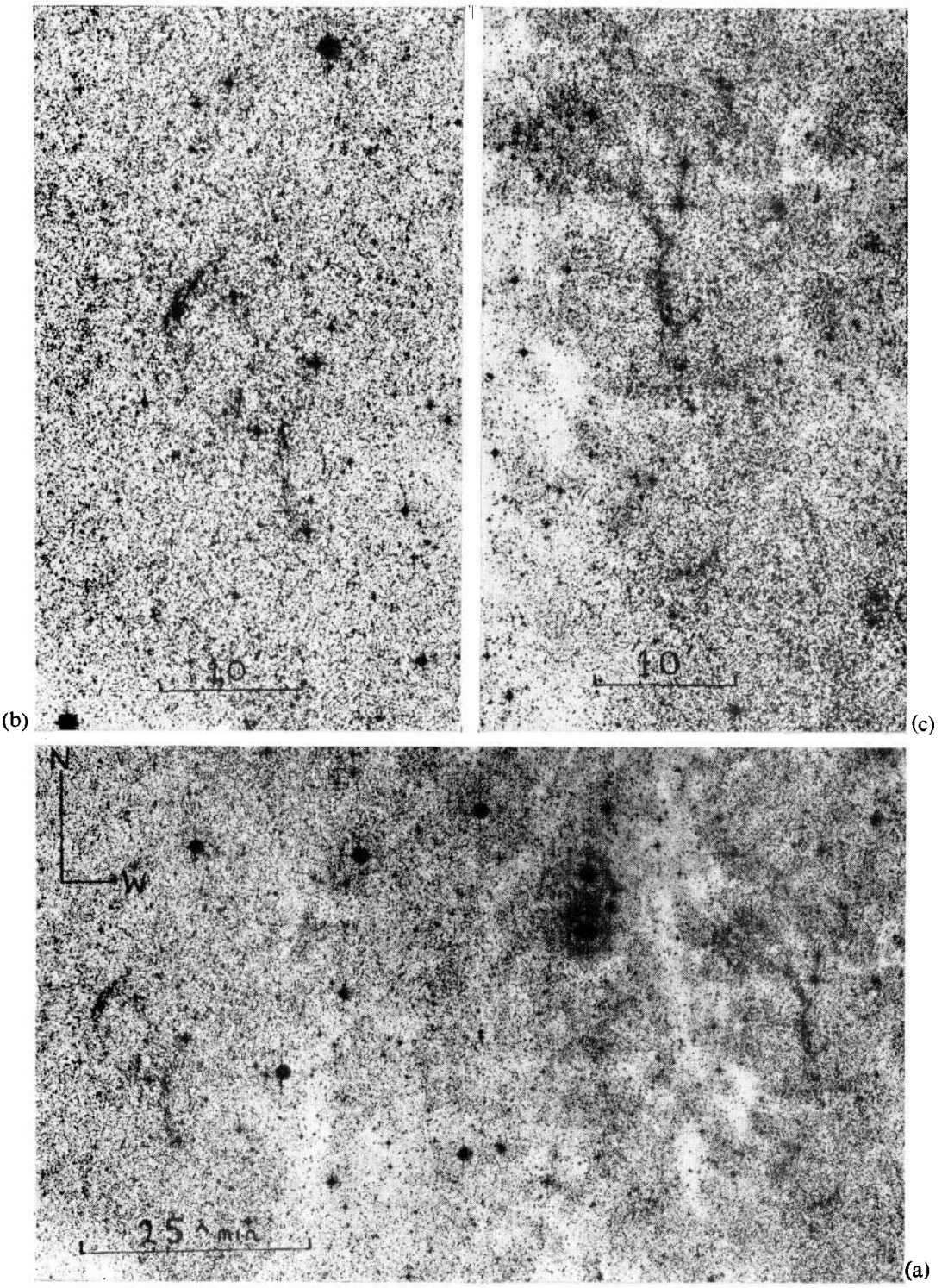

Plate 1. (a) High contrast print of the whole of the W50 region taken from a UKSTU IIIaF-RG630 plate, taken on 1979 June 3. (b) Enlargement of the area around the eastern filament of W50. (c) Enlargement of the area around the western filament of W50.

[*facing page* 736]

1980MNRAS.192..731Z

If this theory is applicable to W50, we find for the observed log (r major/r minor) = 0.35 that $u = 25$. Substituting for α, β we therefore have:

$$\frac{\dot{M}_*(0)V_* r}{(1-\beta^2)^{1/2}E_0} = 3.5$$

where $\dot{M}_*(0)$ is the rest mass loss rate per steradian, $\beta = V_*/C$ and E_0 is the total explosion kinetic energy.

We must now substitute our estimate of r. Rather than adopting a particular value, we will carry through the argument using two values of the distance, 2 and 6 kpc, giving the 6 kpc estimates in parentheses.

Substituting $\beta = 0.27$, $r = 20.5$ (61.5) pc we have:

$$\dot{M}_*(0) = 7.4(25.4) \times 10^{-6}\,\Omega \left(\frac{E_0}{10^{50}\,\mathrm{erg}}\right) M_\odot\,\mathrm{yr}^{-1} \tag{3.8}$$

where Ω is the solid angle swept out by the beams on the interstellar medium. Note that this mass loss estimate is independent of the assumed pre-shock density or age of the system.

This result will break down if W50 is in the radiation dominated phase III of its expansion (Woltjer 1972). This begins when the cooling time becomes shorter than about four times the expansion time. Using a cooling rate Δ, of

$$\Delta = 1.55 \times 10^{-19} T_e^{-0.5} \left(\frac{Z}{Z_\odot}\right) \mathrm{erg\ cm^3\ s^{-1}} \tag{3.9}$$

which is a fair approximation to the Raymond, Cox & Smith (1976) cooling function above 2×10^5 K and using the Sedov (1959) expansion time, we find the critical radius r_c is given by (approximately):

$$\frac{r_c}{\mathrm{pc}} = 13.4 \left(\frac{N_0}{\mathrm{cm^{-3}}}\right)^{-3/7} \left(\frac{E_0}{10^{50}\,\mathrm{erg}}\right)^{+2/7} \left(\frac{Z}{Z_\odot}\right)^{-1/7} \tag{3.10}$$

where $Z/Z_\odot$ is the abundance of the iron peak elements (which dominate the cooling) compared with the solar value. Once this point is reached, the radius, $r \propto t^{1/4}$ and so a rapid increase in asymmetry of the resultant shell will set in. The development in time of the ansae is then entirely dominated by the stellar wind pressure and morphology cannot be used to derive the mass loss.

The density N_0 is not known, but a reasonable guess is in the range $1.0 > n > 0.1$ cm^{-3}. Since E_0 is probably of order 6×10^{50} erg, the critical radius r_c is between $60 \geqslant r_c \geqslant 23$ pc. The mass loss estimate (3.8) can therefore be regarded as giving an upper limit.

3.2 STELLAR WIND ONLY

In view of the mechanical energy which can be delivered by the relativistic jets of SS433, it is not unreasonable to ask if these alone can account for W50. In this model, the jets act on the interstellar medium somewhat like a high speed water jet on a pile of sand, eating into the undisturbed ISM and splashing back from the 'work surface' (Rees 1978) to fill and expand by thermal pressure the cavity about SS433. In this model, the advance of the work surface is given only by the second term of equation (3.5) so that:

$$r^2 = 2\left(\frac{4\dot{M}_* V_*}{3\rho_0}\right)^{1/2} t. \tag{3.11}$$

If we assume that the thermal pressure of the shocked relativistic wind alone inflates the inner elliptical shell, then in an adiabatic approximation the driving pressure is

$$P = \frac{3(\gamma - 1)}{4\pi r^3} E(t). \tag{3.12}$$

Where $E(t)$ is the total thermal energy deposited in the cavity radius r

$$E(t) \approx \frac{9\Omega}{32} \dot{M}_* V_*^2 t. \tag{3.13}$$

Substituting equations (3.13) and (3.12) into equation (3.1) and integrating we have

$$r^5 = \left(\frac{5}{3}\right)^2 \left(\frac{9\Omega(\gamma - 1)\dot{M}_* V_*^2}{32\pi\rho_0}\right) t^3. \tag{3.14}$$

This is the solution for the minor axis $r_{\min}$, whilst (3.11) gives the major axis so:

$$\left(\frac{r_{\max}}{r_{\min}}\right)^5 = 74.3 \left(\frac{\dot{M}_* V_*}{\rho_0}\right)^{1/2} (\Omega V_* r_{\max})^{-1}. \tag{3.15}$$

Substituting for V_* we have:

$$\epsilon^5 = \left(\frac{r_{\max}}{r_{\min}}\right)^5 = 0.47 \left(\frac{\dot{M}_*(0)}{10^{-5} M_\odot \text{ yr}^{-1}}\right)^{1/2} \left(\frac{N_0}{\text{cm}^{-3}}\right)^{-1/2} \left(\frac{r_{\max}}{10 \text{ pc}}\right)^{-1} \Omega^{-1}. \tag{3.16}$$

As can be seen from equation (3.16), any estimate of mass loss will be very much affected by an error in the measurement of the eccentricity of the shell ϵ.

Substituting $r_{\max}/r_{\min} = 2.4$ and $r_{\max} = 35(96)$ pc we have:

$$\dot{M}_*(0) = 0.47(1.42) \left(\frac{N_0}{\text{cm}^{-3}}\right) \Omega^2 M_\odot \text{ yr}^{-1} \tag{3.17}$$

which is unreasonably high for any reasonable choice of Ω or N_0. The reason for this can be seen by inspection of equation (3.15), which shows that the eccentricity varies as $1/r_{\max}^{1/5}$ so low eccentricity occurs only in old systems, and a double lobe structure would dominate at earlier times. In the case of W50, the inner radio shell and optical filaments show that a lobe structure has been a more recent development, in agreement with the SNR plus stellar wind model above but not the present model, where the shocked stellar wind is insufficient to inflate the inner cavity.

However, the shocked stellar wind could explain the relatively 'filled' radio structure. The spectral index α of radio emission from relativistic electrons produced in a shock is $\alpha = -3/2(x-1)^{-1}$ where x is the compression factor. For an adiabatic shock $x = 4$ so $\alpha = -0.5$, very nearly equal to the index observed $\alpha = -0.48$.

This suggests a young population of relativistic electrons, acceptable on this model since electrons generated near the 'work surface' in the relativistic shock can easily fill a cavity generated by a SNR within their radiative lifetimes. The radio emission is then the result of constant replenishment of the relativistic electrons, so we expect on this model that W50 should now have a greater surface brightness than implied from its diameter even if it were originally a normal SNR. This is an indirect argument for accepting a larger distance estimate for the system.

3.3 ASYMMETRY OF THE ANSAE

A striking feature of the radio map is the disparity between the eastern and western ansae, the eastern being more extended and of lower surface brightness. This asymmetry is present, but less marked, in the optical filaments. If interpreted as the result of the decline of gas density above the plane we can obtain an estimate of the distance on the stellar wind model. Equation (3.5) now takes the form:

$$\frac{dr}{dt} = \frac{4\dot{M}_* V_*}{3\rho_0 r^2 \exp\,[-r/H]}; \quad H = h/\cos\,\psi \tag{3.18}$$

where h is the Z scale-height of the gas distribution and ψ is the angle between the radius vector and the normal out of the plane.

For two beams propagating in opposite directions for the same total time, integration of equation (3.18) gives

$$\begin{aligned} &2 - \exp\,[-\zeta_u](\zeta_u^2 + 2\zeta_u + 2) \\ &\quad = -2 + \exp\,[\zeta_L](\zeta_L^2 - 2\zeta_L + 2) \\ &\quad = \frac{4\dot{M}_* V_* t}{3\rho_0 H^3} \end{aligned} \tag{3.19}$$

where ζ_u and ζ_L are the distances, measured from the mass loss centre of the upper and lower ansae respectively. In Fig. 4 we plot the dimensionless time τ, $(4\dot{M}_* V_* t/3\rho_0 H^3)$, against the dimensionless radius ζ for the upper and lower ansae. Note that, as in the case of the Kompaneets solution for a supernova explosion in an exponential atmosphere, the upper ansae moves off to infinity at finite time ($\tau = 2$). At this τ the lower ansae is at $\zeta_L = 1.300075$ which may be compared to the SNR case where the equivalent $\zeta_L = 1.38$.

From the observed ratio ζ_u/ζ_L, we derive from Fig. 4 a value of $\zeta_u = 0.66$ which implies a scale height $h = 1.51°$. Since a probable value of h is between 130 and 160 pc, this gives a distance of between 5 and 6 kpc for SS433/W50.

4 A cloudlet shock model for the optical filaments

Despite the very low velocity dispersion in the optical filaments, the very great strength of the [S II] and [O I] lines makes it almost certain that these arise in a low velocity shock,

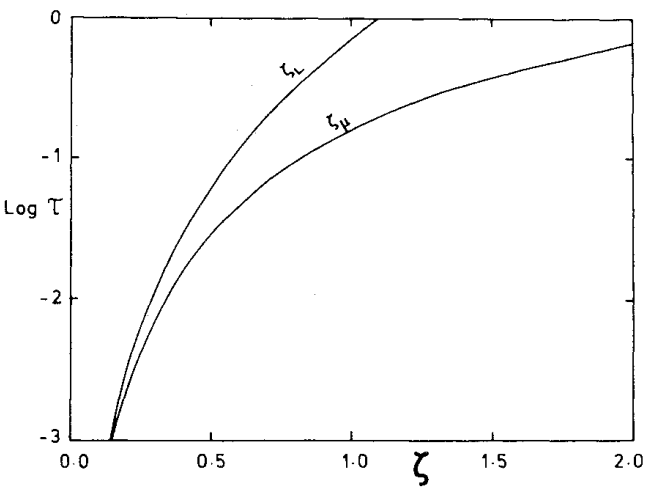

Figure 4. Propagation of the ansae in an exponential density gradient. τ is the dimensionless time and ζ the dimensionless distance. The curves labelled ζ_u and ζ_L refer to the upper and lower ansae respectively.

which the figures in Table 3 suggest to be around 40–60 km s^{-1}. An upper limit for the shock velocity is obtained if we assume the shocks travel in the same direction as the relativistic beams, at 78° to the line-of-sight. Since the velocity difference between the east and west is 44 km s^{-1}, the shock velocity must therefore be less than 106 km s^{-1}.

Although an anomalous abundance is suggested by the spectra, this is not absolutely essential except perhaps for nitrogen, and indeed, the spectra bear a close resemblance to the class of low excitation Herbig–Haro objects such as HH-7 and HH-11 (Böhm, Brugel & Mannery 1980) for which simple radiative shock models (Dopita 1978) do not give a good account. Furthermore, it has been recently demonstrated (Schwartz & Dopita 1980) that the most likely mode of excitation is by the ram pressure of a stellar wind driving a slow shock into dense cloudlets, and shock velocities of order 40–50 km s^{-1} are indicated for the low excitation objects.

We therefore consider a cloudlet shock model to produce the optical emission in W50. If N_w, δ_w are the density, and ratio of specific heats in the wind and N_c, δ_c the corresponding variables in the cloudlet then (McKee & Cowie 1975):

$$N_c V_c^2 = \frac{\delta\gamma_c + 1}{\gamma_w + 1} N_w V_w^2,$$

where

$$\delta = 3.15 - 4.78x + 2.63x^2$$

$$= \frac{\gamma_w + 1}{\gamma_c + 1} \frac{V_c}{V_w} \tag{4.1}$$

and V_w, V_c are respectively the wind velocity and the velocity of the cloudlet shock. Equation (4.1) shows that the pressure driving the cloudlet shock can be enhanced by a factor 3.15 over the ram pressure of the wind, which will be the case in W50. The cloudlets would then be surrounded by a stand-off shock in the outflowing relativistic gas, and so the flux of cosmic rays and high-energy photons generated in the shocked layer might therefore be expected to produce somewhat unusual conditions in the shocked cloudlet gas.

In the previous section we found that the ram pressure of the wind is much larger than the pressure driving the SNR ($u = 25$). This result is supported by the non-observability of filaments associated with the main shell of the remnant; since the optical emission scales as the driving pressure the pressure in the ansae must indeed be higher by a factor of order 10 than in the main shell. We therefore neglect any component of pressure due to the SNR.

The pressure driving the cloudlet shock, P_c, can be found from the observed [S II] ratio. If N[S II] is the density indicated by the [S II] lines, then the shock-wave theory developed by Dopita (1978) gives (provided magnetic field terms are negligible):

$$P_c = (1.9 \pm 0.7) \times 10^{-9} \left(\frac{N[\text{S II}]}{10^3 \text{ cm}^{-3}}\right) \text{dyne cm}^{-2}. \tag{4.2}$$

By use of equation (4.1) and equating the pressure to (3.4) we therefore derive the result:

$$\dot{M}_*(0) = 1.1 \times 10^{-6}\, \Omega \left(\frac{r}{10 \text{ pc}}\right)^2 \left(\frac{N[\text{S II}]}{10^3 \text{ cm}^{-3}}\right) M_\odot \text{ yr}^{-1} \tag{4.3}$$

where V_* has been assumed to be 0.27 c.

Although the eastern observation gives an [S II] ratio at the low density limit, for the position Nos 2 and 3 in the west we have N[S II] = 3×10^3 and 1.2×10^3 cm^{-3} respectively.

It is interesting to note that these translate, for an assumed shock velocity of 50 km s^{-1}, to pre-shock densities of 300 and 120 respectively. Such densities are consistent with the idea that the optical filaments have their origin in an earlier shocked and compressed supernova remnant shell, since they are much higher than would be expected for an undisturbed interstellar medium.

Using a value of $r = 18(55)$ pc and adopting $N[\mathrm{S\,II}] = 2.1 \times 10^3$ we have from equation (4.3):

$$M_*(0) = 6.8(63) \times 10^{-6}\,\Omega\,M_\odot\ \mathrm{yr}^{-1}. \tag{4.4}$$

This figure is believed more reliable than (3.8). Since $E_0 \approx 6 \times 10^{50}$ erg (Dopita 1979) and equation (3.8) is an upper limit we conclude that

$$\underset{(150 \times 10^{-6})}{41 \times 10^{-6}\,\Omega} > \dot{M}_*(0) \gtrsim \underset{(63 \times 10^{-6})}{7 \times 10^{-6}\,\Omega}\,M_\odot\ \mathrm{yr}^{-1}.$$

The Sedov (1959) age t can also be estimated:

$$t = 0.922\left(\frac{E_0}{\rho_0}\right)^{-1/2} r^{5/2}$$

which, for an assumed pre-shock density of 0.3 cm^{-3} gives $t = 1.8 \times 10^4\,(2.1 \times 10^5)$ yr.

5 Discussion

In the previous sections we have established, by two entirely separate methods, an estimate of the mass loss in the relativistic beams which is independent of any assumed parameters of the interstellar medium. These estimates can be of vital significance in unravelling the mystery of SS433, and we refer the reader to a recent discussion by Katz (1980).

All our evidence appears to give firm support to a model for SS433 which is the consequence of a normal supernova explosion. This must have occurred in a binary system to give continued activity in relativistic jets, so we look to a solution with accretion in a disc on to a compact object (neutron star or black hole) which is the remnant of the supernova outburst. This accretion disc is certainly gaseous and can probably be associated with the broad (~ 2000 km s^{-1}) Hα emission line about the rest wavelength. Rapid activity in this component is suggested by the observation of a rapidly fluctuating three-component structure in this line (Mathewson & Ford, private communication).

The observed width of the anomalous components limits the angle subtended by the relativistic beams to 0.1 rad, a figure supported by the fact that the angular extent of the ansae and optical filaments is almost the same as twice the precession angle, which limits the beam to an angular width of 0.07 rad. The collimation may be better than this, so a likely value for Ω is of order 0.07 sterad. The estimated mass loss is therefore in the range $3 \times 10^{-6} \gtrsim \dot{M} \gtrsim 5 \times 10^{-7}$ $(10 \times 10^{-6} \geqslant \dot{M} \geqslant 4 \times 10^{-6})\,M_\odot\ \mathrm{yr}^{-1}$ with a probable value around $3 \times 10^{-6}\,M_\odot\ \mathrm{yr}^{-1}$, or approximately $8 \times 10^{-2}\,M_\odot$ in the lifetime of the system.

A mass loss rate of order 1.8×10^{20} g s^{-1} implies a mechanical luminosity ($L_\mathrm{m} = \dot{M}_* V_*^2/2$) of order 6.5×10^{39} erg s^{-1}.

Compare this with the Eddington luminosity for critical accretion on to a black hole (Rees 1978; Lynden-Bell 1978)

$$L_\mathrm{edd} \approx 1.3 \times 10^{38}\,(M/M_\odot)\ \mathrm{erg\ s}^{-1}.$$

The mechanical luminosity derived implies (for a black hole model) critical accretion on a black hole of mass $50\,M_\odot$. A more probable scenario would be supercritical accretion from a

binary companion on to a black hole or neutron star. A very readable account of this problem has been recently given by Jaroszyński, Abramowicz & Paczyński (1980). In their model, a thick disc forms a funnel about the rotation axis, which is separated by a cusp from an almost flat accretion stream in free fall on to the black hole. Conditions in this region are therefore very suitable for producing highly collimated relativistic jets out along the rotation axis. For acceleration in this region, a terminal velocity of $0.27c$ would be achieved in their models for a luminosity which exceeds the critical value by a factor 4 or 5.

If the central object is a black hole then our mass estimate lies in the vicinity of $12\,M_\odot$ although values as high as $40\,M_\odot$ and as low as $1.9\,M_\odot$ are possible, assuming all the luminosity is converted to mechanical energy of the beams.

Very recently, Martin & Rees (1979) have proposed a model for SS433 in which a black hole of $\sim 5\,M_\odot$ is orbited by a degenerate dwarf companion which fills its Roche lobe. In this, the ~ 160 day precession period is caused by the Lense–Thirring dragging of inertial frames, and gas is released by orbital decay of the binary due to gravitational radiation. In their model, if M_* and M_H are the mass of star and hole respectively, the lifetime of the system

$$\tau = 1.7 \times 10^5 M_*^{3/5} M_H^{-6/5} \text{ yr}$$

and the resulting mass loss is

$$M = 6 \times 10^{-6} M_*^{2/5} M_H^{6/5} M_\odot \text{ yr}^{-1}$$

of which the vast majority is ejected by the system at low velocity and is identified with the rest Hα system.

If this model is correct, the kinetic energy carried from the system by this wind ($\sim 4 \times 10^{37}$ erg s^{-1}) is negligible compared to what we have found for the jets and so will be unimportant in the dynamic evolution of W50.

Since the energy of the jets is comfortably inside the limit of $\lesssim 100\,L_{edd}$ which they propose, and the present lifetime of the system is of the same order of magnitude as the age we compute for W50, we conclude that there is no conflict between our observations and the Martin & Rees model.

An alternative model involving a binary system would involve a compact (or collapsed) object and a non-degenerate companion which supplies the accretion (Roberts 1974). In this case driven precession occurs at an angular rate (Katz 1980) of:

$$\Omega = \frac{r^3 \omega}{R^3} \frac{M_2}{M_1}$$

where ω is the spin angular velocity of the precessing object mass M_1 radius r_1 and M_2 is the mass of the companion at binary separation R. This model has the advantage of providing a source of gas which is predominantly composed of hydrogen. If the compact object is a neutron star, the energy released in accretion will be approximately the gravitational binding energy at the surface or $\lesssim 5$ per cent mc^2. To maintain the mechanical luminosity of the jets the accretion rate would have to be much higher than on to a black hole. Since the neutron star cannot exceed $\sim 2\,M_\odot$ the net rate of accretion M_{ac} required lies in the range:

$$1.2 \times 10^{22} > \dot{M}_{ac} > 0.8 \times 10^{21} \text{ g s}^{-1}.$$

Since in the lifetime of the system, this is of order $3\,M_\odot$, such an accretion rate would have probably induced collapse of the neutron star into a black hole anyway. A further problem with this model is how this rate of accretion could be maintained against its own radiation pressure.

6 Conclusion

The discovery of optical filaments in W50 associated with the relativistic beams of SS433 has provided a means to derive a good estimate for the kinetic energy of gas in these beams. The figures suggest that a normal supernova explosion occurred between 2×10^4 and 2×10^5 yr ago in one of the components of a massive binary system, and that the collapsed remnant of this explosion is now accreting at a supercritical rate from its companion. The collapsed object is more likely to be a black hole than a neutron star. If originally it was a neutron star it has probably been forced into further collapse by the accretion flow.

References

Abell, G. O. & Margon, B., 1979. *Nature,* **279,** 701.
Böhm, K. H., Brugel, E. W. & Mannery, E., 1980. *Astrophys. J.,* **235,** L137.
Boksenburg, A., 1972. *Proc. ESO/CERN Conf. Auxiliary Instrumentation for Large Telescopes*, Geneva, May 2–5, p. 295.
Boksenburg, A. & Burgess, D. E., 1973. *Proc. Symp. Astr. Observation*, Vancouver, May 15–17, p. 21.
Caswell, J. L., 1977. *Proc. astr. Soc. Aust.,* **3,** 130.
Caswell, J. L. & Lerche, I., 1978. *Mon. Not. R. astr. Soc.,* **187,** 201.
Chamberlain, J. W., 1961. *Physics of the Aurora and Airglow*, Academic Press, New York.
Clark, D. H. & Caswell, J. L., 1976. *Mon. Not. R. astr. Soc.,* **174,** 267.
Clark, D. H. & Murdin, P., 1978. *Nature,* **276,** 45.
Clark, D. H., Green, A. & Caswell, J. L., 1975. *Aust. J. Phys. Suppl.,* **37,** 75.
Dopita, M. A., 1978. *Astrophys. J. Suppl.,* **37,** 117.
Dopita, M. A., 1979. *Astrophys. J. Suppl.,* **40,** 459.
Dopita, M. A., Mathewson, D. S. & Ford, V. L., 1977. *Astrophys. J.,* **214,** 179.
Geldzahler, B. J., Pauls, T. & Salter, C. J., 1980. *Astr. Astrophys.,* **84,** 237.
Goss, W. M., Shaver, P., Zealey, W. J., Murdin, P. & Clark, D. H., 1979. *Mon. Not. R. astr. Soc.,* **188,** 357.
Jaroszyński, M., Abramowicz, M. A. & Paczyński, B., 1979. *Astr. Astrophys.,* in press.
Katz, J. I., 1980. *Astrophys. J.,* **236,** L127.
Kompaneets, A. S., 1960. *Dokl. Acad. Nauk. SSSR,* **130,** 1001.
Large, M. I., 1970. *Astrophys. Lett.,* **5,** 11.
Longmore, A. J., Clark, D. H. & Murdin, P., 1977. *Mon. Not. R. astr. Soc.,* **181,** 541.
Lynden-Bell, D., 1978. *Phys. Scripta,* **17,** 185.
McKee, C. F. & Cowie, L. L., 1975. *Astrophys. J.,* **195,** 715.
Malin, D. F., 1977. *Am. astr. Soc. Photobull.,* **16,** 14.
Malin, D. F., 1978. *Nature,* **276,** 591.
Margon, B., Ford, H. C., Katz, J. I., Kwitter, K. B., Ulrich, R. K., Stone, R. P. S. & Klemola, A., 1979. *Astrophys. J.,* **230,** L41.
Martin, P. G., Murdin, P. & Clark, D. H., 1979. *IAU Circ., No. 3358.*
Martin, P. G. & Rees, M. J., 1979. *Mon. Not. R. astr. Soc.,* **189,** 19P.
Milne, D., 1979. *Aust. J. Phys.,* **32,** 83.
Murdin, P. & Clark, D. H., 1979. *IAU Circ., No. 3400.*
Oke, J. B., 1974. *Astrophys. J. Suppl. Ser.,* **27,** 21 (No. 236).
Raymond, J. C., Cox, D. P. & Smith, B. W., 1976. *Astrophys. J.,* **204,** 290.
Rees, M. J., 1978. *Phys. Scripta,* **17,** 193.
Roberts, W. J., 1974. *Astrophys. J.,* **187,** 575.
Ryle, M., Caswell, J. L., Hine, G. & Shakeshaft, J., 1978. *Nature,* **276,** 571.
Schwartz, R. D. & Dopita, M. A., 1980. *Astrophys. J.,* **236,** 543.
Sedov, L., 1959. *Similarity and Dimensional Methods in Mechanics,* Academic Press, New York.
van den Bergh, S., 1979. *IAU Circ. No. 3393.*
Velusamy, T. & Kundu, M. R., 1974. *Astr. Astrophys.,* **32,** 375.
Woltjer, L., 1972. *A. Rev. Astr. Astrophys.,* **10,** 129.
Zealey, W. J., Elliott, K. H. & Malin, D. F., 1979. *Astr. Astrophys. Suppl.,* **38,** 39.